Desalination and Water Treatment
www.deswater.com

doi: 10.5004/dwt.2021.27590

234 (2021) 234–244
September

Optimization of synthetic dyes removal from wastewaters using loofah biomaterial: equilibrium, kinetic, and thermodynamic studies

Faiza Benaissa*, Hamida Maachou, Mohamed Nedjhioui

Laboratory Materials and Environment, Medea University, Medea, Algeria, Tel. +213-25785133; Fax: +213-25785628; emails: benaissaf@ymail.com/benaissa.faiza@univ-medea.dz (F. Benaissa), hamidamaachou@yahoo.fr (H. Maachou), nedjhioui@gmail.com (M. Nedjhioui)

Received 16 March 2021; Accepted 5 July 2021

ABSTRACT

In this study, loofah was used to remove organic dyes (crystal violet, methylene blue, and basic fuchsine) from an aqueous solution by biosorption. The effects of operating parameters, such as contact time, initial pH, dyes concentration, size of biosorbent and temperature, on the discoloration yields were evaluated. The experimental results revealed that the highest removal efficiencies of crystal violet, methylene blue, and basic fuchsine were 99.5%, 98.66%, and 85%, respectively, at the optimum conditions (operating time of 60 min, initial pH (6.92 for the crystal violet, 6.60 for methylene blue and 8.53 for basic fuchsine), dyes concentration of 6 mg/L, size of loofah squares $S = 16$ cm^2 and temperature of 60°C). The structural characterization of the loofah after biosorption of dyes using Fourier-transform infrared spectroscopy analysis showed an intensity reduction of the characteristic peaks of the hydroxyl groups and the apparition of novel characteristic peaks of amine groups indicating thus the fixation of dyes on loofah. Equilibrium isotherms models showed that the Langmuir isotherm model gives the best fit for the experimental data with the best regression coefficient $R^2 > 0.99$. Adsorption kinetics showed that the biosorption followed a pseudo-second-order reaction. Thermodynamic study indicates an endothermic process with physical nature.

Keywords: Biosorption; Dye; Isotherm; Kinetic; Loofah; Thermodynamic

1. Introduction

Dyes have discovered many packages in industries which including textile, paper, rubber, plastic, leather, cosmetic, pharmaceutical, and meals processing [1,2]. Effluents from these industries contain various types of artificial dyes [3]. The increase in the polluting dyes in the environment is a dangerous threat to the ecosystem and public health. To remedy this problem, industrial effluents must be treated before their discharge [4–6].

Recently, several physicochemical methods have been used to remove dyes from aqueous media such as photocatalytic degradation [7], coagulation and ultrafiltration [8], oxidative degradation [9], adsorption [10], and other electrochemical methods [11–13]. Biosorption is considered to be a more economical and efficient method owing to the simplicity of design, the availability and the ability to process the dyes in a more concentrated form and provide a sludge-free solution [14,15].

Various inexpensive adsorbents derived from agricultural wastes or natural materials have been extensively studied for the removal of dyes from aqueous solutions. Many researchers have studied the use of cheap and effective alternative substitutes to remove dyes from wastewater. Some of these alternative adsorbents are palm ash and chitosan/palm oil ash [16,17], shale oil ash [18], grapefruit bark (*Citrus grandis*) [19], deoiled soybeans and bottom ash [20], sunflower seed shells and mandarin peelings

* Corresponding author.

1944-3994/1944-3986 © 2021 Desalination Publications. All rights reserved.

[21], wheat husks [22,23], powdered guava leaves [24] and wastes from the steel and fertilizers [25]. However, new economic, available, eco-friendly and effective adsorbents are still being sought. *Luffa cylindrica* can offer a new alternative adsorbent due to its availability, low cost, biodegradability, and micro-capillary structure. Known as sponge squash and cylindrical loofah, it belongs to the Cucurbitaceae family [26]. It consists of cellulose, hemicelluloses and lignin [27]. Therefore, it has a fibrous vascular system [28] which facilitates the elimination of pollutants from water. Few researchers have used cylindrical loofah in distinctive shapes to eliminate dyes from the solution. While Abdelwahab [29] used activated charcoal loofah, Demir et al. [27] used loofah handled with NaOH and Oladoja et al. [30] used untreated loofah to eliminate dyes from the solution. The study aims to valorize the *Luffa cylindrica* biomaterial, and evaluate its performance in the elimination of organic dyes (violet crystal, methylene blue, and basic fuchsine) in an aqueous solution by biosorption. Various parameters affecting dyes biosorption such as contact time, initial pH, dyes concentration, and temperature were studied and discussed. Isotherms, kinetics, and thermodynamic studies were also investigated.

2. Materials and methods

2.1. Preparation of biosorbent

Algerian cylindrical loofah (Fig. 1a) is first thoroughly washed with distilled water at 80°C for 2 h to clean the adhering dust. It was oven-dried at 40°C for 3–4 h. After drying, it was cut into small squares of 16 cm^2 to be used as shown in Fig. 1b.

2.2. Used adsorbates

Crystal violet l, methylene blue, and basic fuchsine with 95% purity (obtained from Isma Dye Company) were chosen as adsorbate and were used without any purification.

2.3. Biosorption procedure

Biosorption studies have been executed at room temperature (25°C) using 250 mL vials. Each vial contained 100 mL of dye solution (in the range of 6–100 mg/L) and a weighed amount of biosorbent. pH studies were conducted between 2 and 9 to determine the optimal pH at which maximum color removal could be achieved. pH was adjusted to the desired value by adding either a few drops of hydrochloric acid or sodium hydroxide solution. The effect of the biosorbent size on the rate of discoloration was studied for initial concentrations of 6 mg/L for each dye, a contact time of 60 min, an initial dye volume of 100 mL, and at natural pH of each dye. The effect of temperature on the yields of dyes discoloration was studied at three constant temperatures of 25°C, 40°C, and 60°C, with dye solutions volume of 100 mL, an initial concentration of 6 mg/L, an adsorbent surface of 16 cm^2, and at the natural pH of each solution. All solutions are immersed in a thermostat bath to keep the desired temperature constant.

After each experiment, the final concentration of dye in the solution was measured by a UV-vis spectrophotometer (Model: SHIMADZU, UV mini-1240) at a wavelength of 586 nm for the crystal violet, 574 nm for the basic fuchsine, and 676 nm for the methylene blue using a calibration curve. The amount of the dye removed from the solution was calculated by Eq. (1).

$$\%\text{Removal} = \left[\frac{C_0 - C_t}{C_0}\right] \times 100 \tag{1}$$

where C_0 (mg/L) is the initial dye concentration and C_t (mg/L) is the dye concentration at time t.

The biosorption capacity q_e (mg/g) was calculated by the mass balance relationship:

$$q_e = \left[\frac{C_0 - C_e}{W}\right] \times V \tag{2}$$

where C_0 (mg/L) is the initial dye concentration and C_e (mg/L) is the equilibrium liquid-phase concentration of dye, V is the solution volume (L), and W is the weight of the dry biosorbent used (g).

2.4. Fourier-transform infrared spectroscopy analysis

Attenuated total reflection FTIR spectroscopy analysis on the dried biosorbents, before and after biosorption, was carried out with a FTIR-8400 infrared spectrophotometer (Shimadzu-Japan) from 4,000 to 400 cm^{-1}.

2.5. Equilibrium studies

The adsorption equilibrium is generally represented by the adsorption isotherms, giving the relationship between

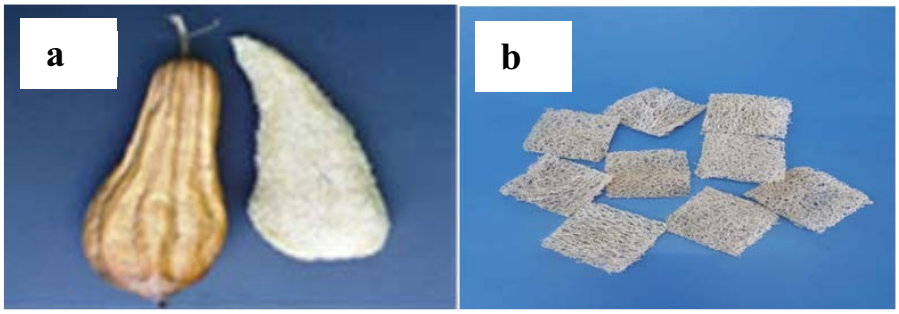

Fig. 1. Photograph of: loofah sponge (a) and squares of loofah (b).

the adsorbate's amount fixed on the solid and its concentration in the liquid or gas phase. In this study, Langmuir, Freundlich, Temkin, and Dubinin–Radushkevich adsorption isotherm were used to predict the biosorption of dyes on loofah.

The Langmuir isotherm is applied for monolayer adsorption onto a surface containing identical binding sites with a finite number [31]. The linearized expression of Langmuir isotherm can be given as:

$$\frac{C_e}{q_e} = \frac{1}{q_m b} + \frac{C_e}{q_m} \tag{3}$$

where q_m is the maximum adsorption capacity, b is a coefficient related to the sorbate affinity to the sorbent, q_e is the quantity adsorbed at equilibrium concentration C_e. The viability of adsorption can also be defined from the dimensionless separation factor R_L given by Eq. (4) [32].

$$R_L = \frac{1}{1 + bC_0} \tag{4}$$

where C_0 is the initial concentration of adsorbate (mg/L), and b (L/mg) is the Langmuir constant. The R_L value indicates either unfavorable ($R_L > 1$), linear ($R_L = 1$), favorable ($0 < R_L < 1$), or irreversible ($R_L = 0$) adsorption.

The Freundlich isotherm model involves heterogeneous surfaces in which the adsorption sites are exponentially distributed with respect to the adsorption heat. The linear form of Freundlich isotherm may be represented as follows [33]:

$$\log q_e = \log K_f + \frac{1}{n}\log C_e \tag{5}$$

where K_f indicates the adsorption capacity and n indicates the adsorption intensity. The value of n indicates the favorability of adsorption. Values of $n > 1$ represent a favorable adsorption.

The Temkin isotherm has generally been applied in the following linear form [34]

$$q_e = B\ln A + B\ln C_e \tag{6}$$

$$B = \frac{RT}{b} \tag{7}$$

where A (L/g) is the Temkin isotherm constant, B is a constant related to adsorption heat, R is the gas constant (8.314 J/mol K), T is the temperature (K) and b is related to the adsorption heat (J/mol).

The Dubinin–Radushkevich (D–R) isotherm model was used in order to deduce the heterogeneity of the surface energies of adsorption and the characteristic porosity of the adsorbent as reported by Dubinin et al. [35]. The linear form is given by Eq. (8).

$$\ln q_e = \ln q_D - B\varepsilon^2 \tag{8}$$

where q_D (mg/g) represents the theoretical saturation capacity, B is a constant dependant on the free energy of biosorption per mole of the adsorbate (mol²/J²) and ε is the Polanyi potential which is related to equilibrium as follows [35]:

$$\varepsilon = RT\ln\left(1 + \frac{1}{C_e}\right) \tag{9}$$

where R is the gas constant (8.314 J/mol/K) and T (K) is the temperature. The mean sorption energy (E) is calculated using the following relation.

$$E = \frac{1}{\left(2B\right)^{1/2}} \tag{10}$$

2.6. Kinetic studies

The kinetic adsorption data were processed to understand the dynamic of adsorption process in terms of the order of rate constant [16]. In this study, four kinetic models were used:

The pseudo-first-order model is expressed by Eq. (11) [36]:

$$\log\left(q_e - q_t\right) = \log q_e - K_1\frac{t}{2.303} \tag{11}$$

Values of K_1 (min⁻¹) can be deduced from the slope of the plot of $\log(q_e - q_t)$ vs. t.

The pseudo-second-order kinetic model is expressed by Eq. (12) [37]

$$\frac{t}{q_t} = \frac{1}{K_2 q_e^2} + \frac{1}{q_e}t \tag{12}$$

The Elovich equation is another rate equation in which the absorbing surface is heterogeneous. It is generally expressed by Eq. (13) [38]

$$q_t = \frac{1}{\beta}\ln\left(\alpha\beta\right) + \frac{1}{\beta}\ln t \tag{13}$$

where α is the initial adsorption rate (mg/g min), β (g/mg) is related to the extent of surface coverage and the activation energy for chemisorption.

The adsorption of dyes can be controlled via external film diffusion in the beginning and by the particle diffusion later. The intra-particle diffusion model is expressed by Eq. (14) as reported in the literature [39].

$$q_t = K_{\text{dif}}t^{1/2} + C \tag{14}$$

where K_{dif} is the intra-particle diffusion rate constant (mg/(g min$^{1/2}$)), C is the intercept. The rate constant K_{dif} was directly evaluated from the slope of the regression line of q_t vs. $t^{1/2}$ plots.

2.7. Thermodynamic studies

The thermodynamic parameters (Gibbs energy (ΔG), enthalpy (ΔH), and entropy (ΔS)) of biosorption are calculated from the data generated by conducting the dyes

biosorption process at several temperatures. These biosorption parameters, ΔH, ΔS, and ΔG, were deduced from the $\log K_d$ vs. $1/T$ plots using Eqs. (15) and (16) [40].

$$\log K_d = \frac{\Delta S}{2.303R} - \frac{\Delta H}{2.303RT} \quad (15)$$

$$\Delta G = \Delta H - T\Delta S \quad (16)$$

where $K_d = q_e/C_e$ *is* known as the distribution coefficient, T is the temperature (K), and $R = 8.314$ J K^{-1} mol^{-1}.

3. Results and discussion

3.1. FTIR characterizations of adsorbent

The infrared analysis contributes to reveal the bonding mechanisms associated with biosorption [41]. Adsorption mechanism is identified from covalent compounds present in the biosorbent material which can act as adsorption sites [42]. Fig. 2 shows the difference in the absorption bands of the functional groups in the infrared spectra before and after biosorption. We can see that loofah displayed a number of absorption peaks before and after biosorption of dyes, reflecting the complex nature of the examined material.

Before biosorption of dyes, we observe a broad absorption peak around 3,618 cm^{-1} which indicates the presence of free hydroxyl groups on the surface of loofah. The peak at 1,450 cm^{-1} is assigned to the stretching and bending vibrations of the C–H bond in methyl groups of lignin. The broadband at 1,735 cm^{-1} is attributed to (C=O) stretching of carboxylic groups of hemicelluloses. These results are in fair agreement with an earlier study [43], which reported that the surface of loofah contains carboxyl and hydroxyl groups. Finally, the (C–O–C) vibration of glycosidic rings and the (C–O) stretching of primary alcohol groups are observed as a strong band at 1,026 cm^{-1} with a shoulder at 1,103 cm^{-1} which confirm that the cellulose is the major component of loofah. All of these functional groups can interact with the dye molecules. Similar results were reported in Olaseni et al. [44].

After biosorption of dyes, we can observe a reduction in the intensity of the band at 3,418 cm^{-1} corresponding to O–H bonds of the hydroxyl groups which can be explained by the decrease in the –OH groups available on the loofah fibers following the biosorption of the dyes molecules. The increase of the intensity of 2,924.18 cm^{-1} peak may be due to the contribution of additional methyl groups provided by the different dyes. The weak peak at about 1,651 cm^{-1} indicates the presence of H–O–H bonds (adsorbed water). The appearance of a peak around 1,500 cm^{-1} is attributed to the elongation of the aromatic C=C bonds provided by the dyes. The peak at (1,250–1,300) cm^{-1} is due to the presence of C–N bonds of the amine groups of dyes. A significant reduction in the elongation band at 1,026.16 cm^{-1} is probably due to the contribution of primary alcohol groups to the fixation of dyes on the fibers.

3.2. Effect of contact time on biosorption

The effect of contact time on the biosorption of dyes is shown in Fig. 3a. It's clear that the discoloration yield increases with an increasing contact time and remains

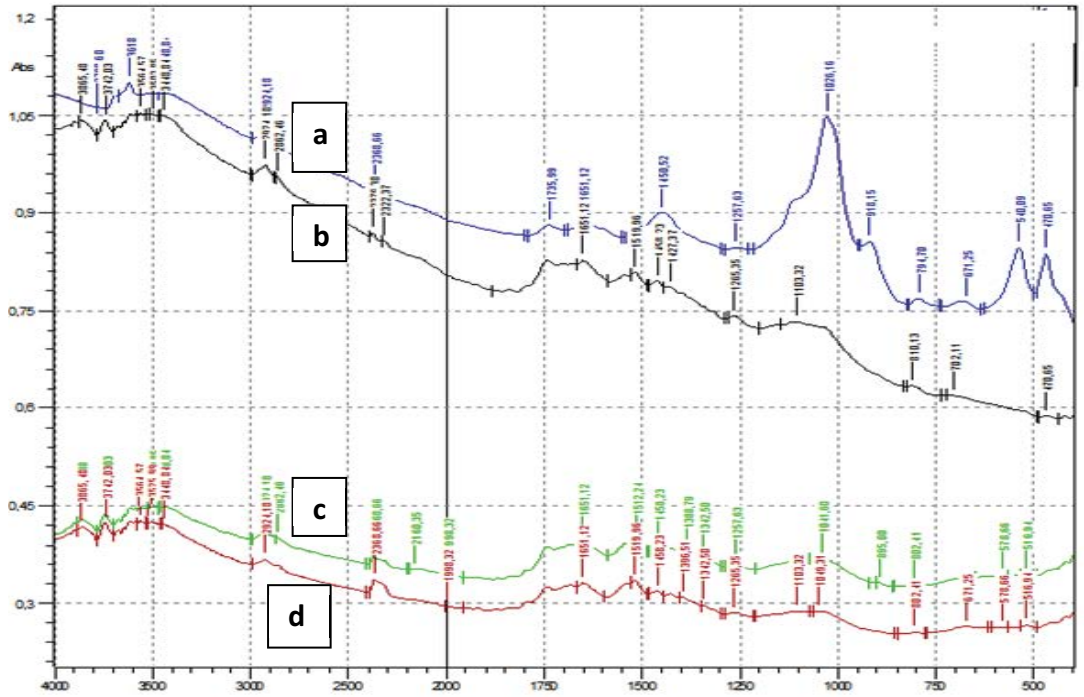

Fig. 2. FTIR spectra of loofah: (a) before biosorption, (b) after biosorption of MB, (c) after biosorption of CV, and (d) after biosorption of BF.

constant after an equilibrium time of 60 min for all dyes. The best discoloration rates reached are 94.3%, 85%, and 84.17% for crystal violet, methylene blue, and basic fuchsine, respectively. After the equilibrium time, the adsorbed amount remains constant, which shows that equilibrium is reached between the bisorbent and the adsorbate. An increase in biosorption capacity with increasing contact time is due to the availability of biosorption sites on the surface of loofah and the equilibrium is explained by the saturation of these sites.

3.3. Effect of initial pH on biosorption

The initial pH is known to be one of the main factors controlling the phenomena of adsorption because it affects the adsorption capacity, dye solubility [45], solution chemistry and the surface of the adsorbent pore [46].

The effect of pH on the biosorption of dyes by loofah is shown in Fig. 3b. The discoloration rate was found to increase with an increasing pH until reaching an optimum biosorption capacity at the natural pH of each dye (pH 6.92 for CV, pH 6.60 for MB, and pH 8.53 for BF). The point of zero charge (pHpzc) of loofah is equal to 5.2 as reported by Olaseni et al. [44], hence its surface is neutral at pH less than 5.2 and negatively charged at pH greater than 5.2. As a result, at pH lower than 5.2, the carboxyl and hydroxyl groups (COOH and OH) on the surface of loofah are protonated making the number of negative charges decrease with a decrease in dyes uptake. Lower biosorption at acid pH was also probably a result of the presence of excess H^+ ions competing with the dye cations for biosorption sites. However, at pH greater than 5.2, the surface of loofah is negatively charged due to the deprotonated functional groups (COO^-) leading to favorable electrostatic or ionic interactions between cationic dyes molecules and loofah. At higher pH, the composition of loofah may be affected (solubilisation of lignins and hemicelluloses) and then the number of active sites decreases which reduces the biosorption capacity. Similar trend was observed for adsorption of methylene blue onto *Posidonia oceanica* (L.) fibres [47].

3.4. Effect of dye concentration on biosorption

The effect of the preliminary dye concentrations on the discoloration yield was studied for concentrations of 6, 10, 20, 40, 60, 80, and 100 mg/L for each dye, the obtained results are illustrated in Fig. 3c. We can see that the discoloration yields for the dyes (CV, MB, and BF) decreases with the increase of their initial concentration. For an initial concentration of 20 mg/L, we note the values of 74%, 73%, and 46% for CV, MB, and BF, respectively. These levels gradually decrease with the increase in the initial concentrations to mark lowers values at 100 mg/L and which are estimated at 20% for MB, 19% for BF, and 48% for CV. At higher concentrations of dyes, molecules tend to aggregate to form large-sized micelles [48]. Consequently, the diffusion of dyes molecules through the micropores of loofah becomes difficult which eliminates intra-particle biosorption of dyes by adsorbent biomaterial. The decrease in biosorption capacity with increasing biosorbent concentration could also be explained by saturation of biosorption sites through the biosorption reaction.

3.5. Effect of biosorbent size on biosorption

The effect of biosorbent size on the biosorption of dyes on loofah was studied; the obtained results are illustrated in Fig. 3d. It is observed that the biosorption capacity increases with increasing size of the biosorbent for the three dyes which can probably due to the greater availability of the biosorption sites or surface area at higher concentration of the biosorbent. The same phenomenon was earlier reported by Yu et al. [49] for the removal of copper from aqueous solutions by sawdust adsorption. For size greater than 16 cm^2, there is a relatively small increase in discoloration rates, this could be explained by the fact that the number of biosorbent sites is greater than the number of dyes molecules. In this case, all the molecules of dyes were biosorbed on loofah and the discoloration yield tend to 100%. Another cause can be due to the splitting impact of concentration gradient between dye molecules and biosorbant concentration causing a decrease in the amount of dye biosorbed onto unit weight of biomass as reported by Malik [50].

3.6. Effect of temperature

The temperature has important effects on the sorption processes. an increase in temperature causes the increase of the diffusion rate for adsorbate molecules within the pores as a result of decreasing solution viscosity and will also modify the equilibrium capacity between adsorbent and adsorbate [51]. The results obtained are illustrated in Fig. 3e. It can be observed that the increase in the temperature from 20°C to 60°C led to an increase in the biosorption capacity of dyes on loofah. The discoloration yields jump from 94%, 85% and 84% for CV, MB and BF at 20°C to achieve the best discoloration yield at 60°C which are estimated at 99.5%, 98.66%, and 85% for CV, BF, and MB, respectively. The increment of biosorption may be due to the increased rate of diffusion of the adsorbate molecules across the surface boundary layer and due to the presence of internal pores in the biosorbent. An increased number of molecules may obtain sufficient energy to succumb an interaction with active sites at the surface. This result indicates that a better biosorption of dye is obtained at higher temperature at the equilibrium time.

3.7. Equilibrium studies

Fig. 4a shows Langmuir plots for the biosorption of CV, MB and BF on loofah. The q_m and R_L constants values and the correlation coefficients are presented in Table 1. The plots were found to be linear with good correlation coefficients (0.99) for CV, MB, and BF. This indicates the applicability of this model for the biosorption of dyes on loofah. Therefore, we can say that the Langmuir isotherm provides a good fit for the experimental data. The maximum adsorbed quantities (q_m), calculated according to the Langmuir model, were all approximately close to experimental values. The dimensionless constant R_L, calculated from Eq. (4), was found to be between 0 and 1 for all dyes used indicating a favorable biosorption process.

According to experimental data, the linear plot of $\log q_e$ vs. $\log C_e$ (Freundlich model) is shown in Fig. 4b. The $1/n$ and K_f values were calculated from the slope and intercept

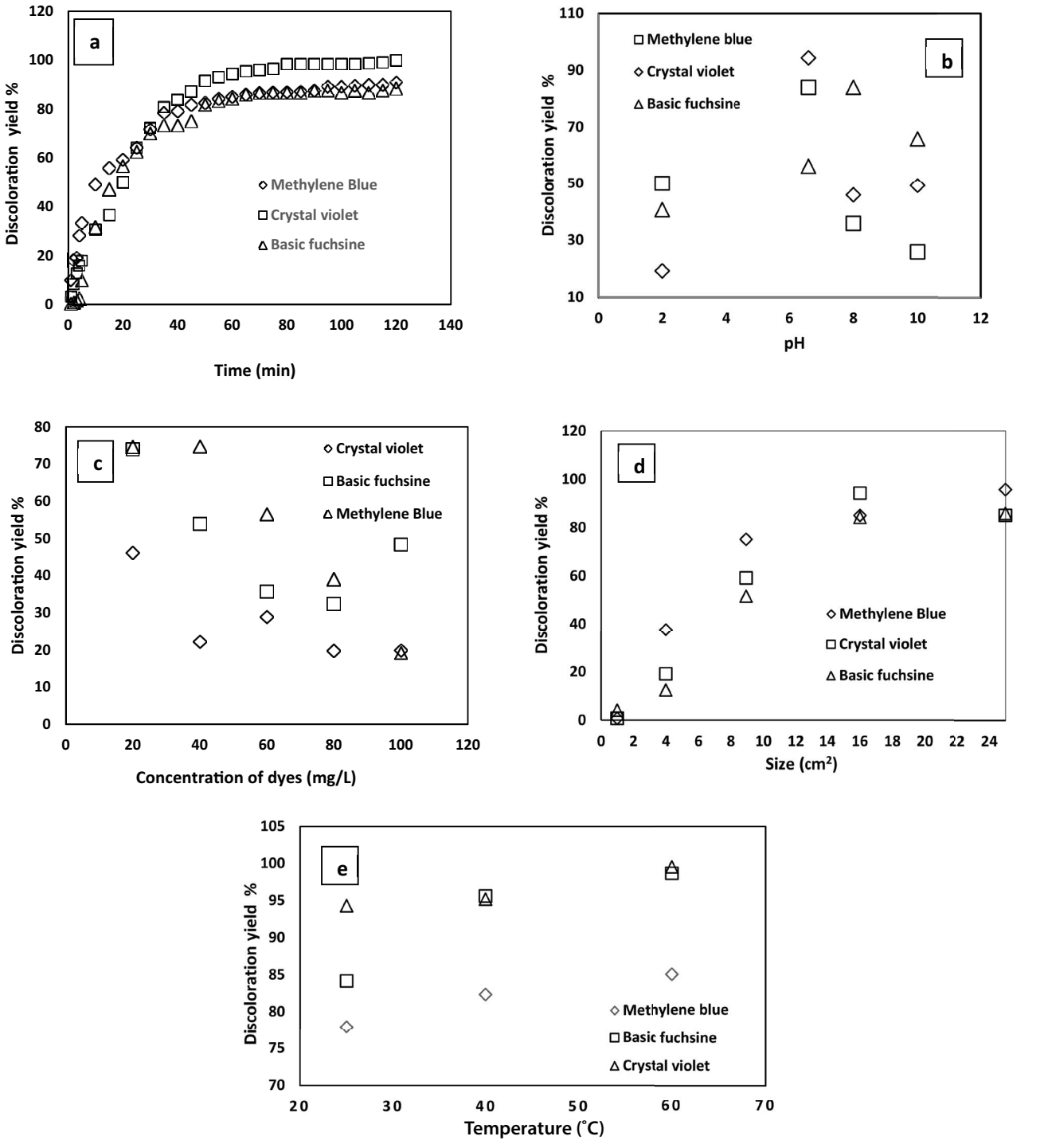

Fig. 3. Effect of experimental parameters on biosorption of dyes on squares of loofah: (a) contact time, (b) initial pH, (c) initial concentration, (d) dimensions of squares of loofah, and (e) temperature.

respectively and they are given in Table 1. As reported in the literature [52], the intensity parameter, $1/n$, indicates the deviation of the adsorption isotherm from the linearity. The adsorption is linear when $(1/n) = 0$, the sites are homogeneous and there is no interaction between the adsorbed species. The adsorption is favorable when $(1/n) < 1$, new adsorption sites appear and the adsorption capacity increases. The adsorption is unfavorable when $(1/n) > 1$, the adsorption bonds become weak and the adsorption capacity decreases. From the obtained results it can be seen that the value of $1/n$ was found to lie between zero and one indicating that CV, MB, and BF dyes are favorably biosorbed by loofah.

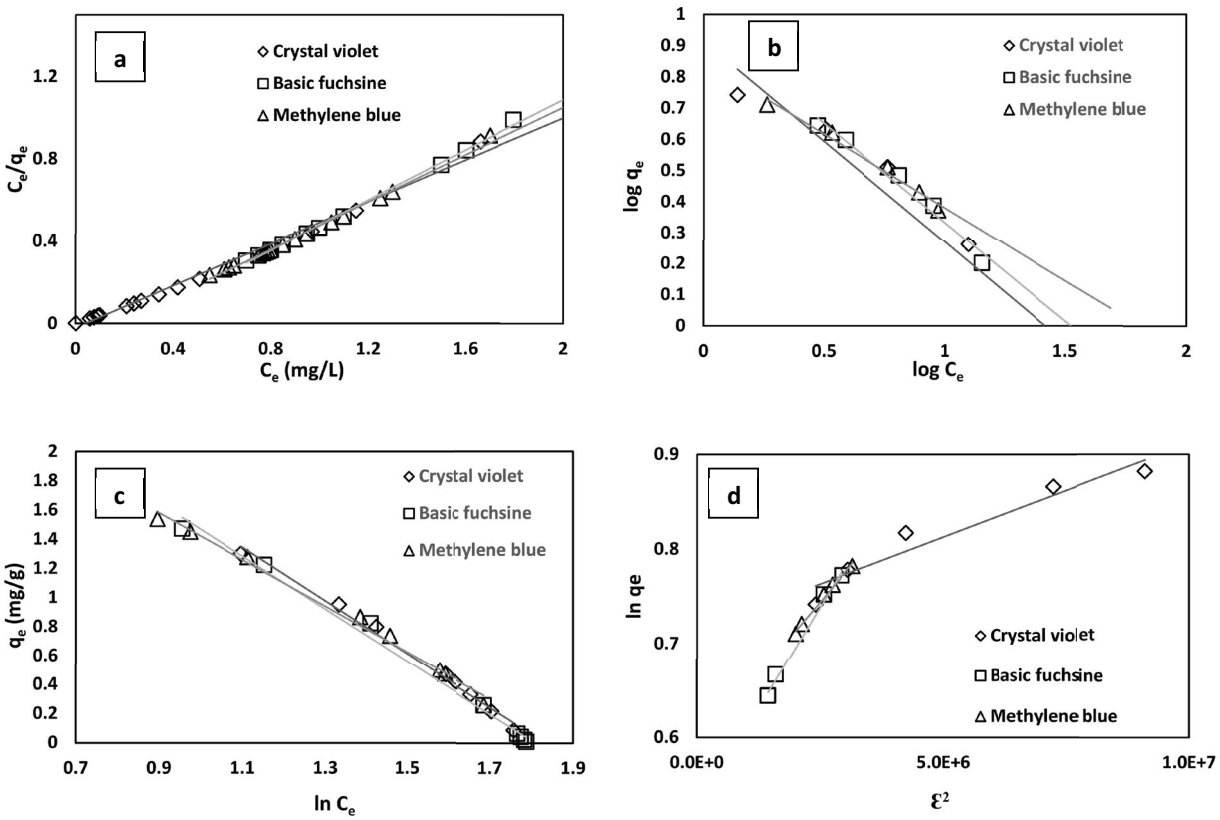

Fig. 4. Isotherm plots for biosorption of dyes on loofah: (a) Langmuir, (b) Freundlich, (c) Temkin, and (d) Dubinin-Radushkevich.

The Temkin plots (Fig. 4c) enables the determination of isotherm constants A and B given in Table 1. According to the regression coefficient R^2 obtained (Table 1), it is seen that this isotherm can be applicable to the description of equilibrium data. The best regression coefficients were observed for all dyes. This result shows that the Temkin model can also describe the biosorption of dyes on loofah.

Finally, the Dubinin–Radushkevich plots ($\ln q_e$ vs. ε^2) for different dyes are shown in Fig. 4d. The calculated Dubinin–Radushkevich constants and mean free energy for adsorption are shown in Table 1. The correlation coefficients (≥90%) for CV, BM, and BF mean that the adsorption of dyes on biosorbent can be described by Dubinin–Radushkevich (DR) model. The theoretical biosorption capacities calculated by this model are relatively close to the experimental values. As reported by Ozcan et al. [53], the energy of activation can predict the nature of adsorption whether it is physisorption or chemisorption. If the energy of activation is less than 8 kJ/mol, the adsorption is physisorption and if the energy of activation is 8–16 kJ/mol, the adsorption is then chemisorption in nature. In this study, the mean adsorption energy was found to be in the range of 2–5 kJ/mol for all dyes used, which are in the energy range of physical adsorption reactions.

Table 1
Constant parameters and correlation coefficients calculated for various isotherm models for adsorption of dyes on loofah (C_0 = 6 mg/L, T = 25°C, initial pH (CV = 6.92, MB = 6.60, BF = 8.53))

Isotherm	Parameters	Dyes		
		MB	CV	BF
Langmuir	q_m (mg g^{-1})	1.74	1.96	1.64
	k_L (L mg^{-1})	5.76	25.34	4.56
	R^2	0.99	0.99	0.99
	R_L	0.03	0.01	0.04
Freundlich	K_f (mg g^{-1})	2.34	2.49	2.63
	$1/n$	0.47	0.64	0.63
	R^2	0.98	0.92	0.97
Temkin	K_t (L mg^{-1})	1.59	1.84	1.81
	ΔQ (kJ mol^{-1})	1.55	1.34	1.36
	R^2	0.91	0.95	0.99
Dubinin–Radushkevich (D–R)	q_m (mg g^{-1})	1.8	2.04	1.68
	$K \times 10^8$ (mol^2 J^{-2})	6	2	9
	E (kJ mol^{-1})	2.88	5	2.35
	R^2	0.98	0.92	0.99

3.8. Kinetic studies

In Fig. 5a, the first-order kinetic model plots were found to be linear with good correlation coefficients (R^2 > 0.90) for all dyes studied. The first-order-rate constants and the regression coefficient values are presented in Table 2. The theoretical q_e (cal) values do not agree with the experimental values q_e (exp) for all dyes studied, these results

Table 2
Constant parameters and correlation coefficient for kinetic models for biosorption of dyes on loofah (C_0 = 6 mg/L, T = 25°C, initial pH (CV = 6.92, MB = 6.60, BF = 8.53))

	Parameters	Dyes		
		MB	CV	BF
Pseudo-first-order	K (min^{-1})	0.0036	0.0043	0.0614
	q_e (cal) (mg g^{-1})	4.72	3.05	2.93
	q_e (exp) (mg g^{-1})	2.44	2.20	2.18
	R^2	0.92	0.98	0.91
Pseudo-second-order	K (min^{-1})	0.62	0.76	0.96
	q_e (cal) (mg g^{-1})	2.55	3.25	2.79
	q_e (exp) (mg g^{-1})	2.44	2.20	2.18
	R^2	0.99	0.98	0.99
Elovich	α (mg g^{-1} min^{-1})	0.65	0.37	0.30
	β (mg g^{-1})	1.80	1.29	1.33
	q_e (exp) (mg g^{-1})	2.44	2.20	2.18
	R^2	0.99	0.96	0.99
Intra-particle diffusion	K_{dif} (mg/(g min$^{1/2}$))	0.17	0.31	0.21
	C	0.81	0.01	0.55
	R^2	0.94	0.91	0.95

imply that the pseudo-first-order kinetic model can't describe the adsorption of dyes on loofah. So, the experimental data were then fitted with the second-order-kinetic model.

The plots of t/q_t vs. t are shown in Fig. 5b. The predictive parameters of linear regression equations and R^2 values of the pseudo-second-order equation are given in Table 2. The plots were found to be linear with the best correlation coefficient for all dyes ($R^2 > 0.99$). The theoretical q_e (cal) values were found to be very close to the experimental q_e (exp) values. Thus, we can say that the second-order-model is in good agreement with experimental data and can be used to describe the biosorption of dyes on loofah with a better fit of experimental data than the pseudo-first-order model.

The Elovich model is represented in Fig. 5c. A plot of q_t vs. ln$t$ gives a linear curve with a slope of (1/β) and an intercept of (1/β)ln(αβ). The Elovich parameters constants and the regression coefficient values are presented in Table 2. We can see from Fig. 5c that the plots are linear. However, comparing the value of coefficient regression, the theoretical and the experimental adsorption capacities (Table 2), we can deduce that the pseudo-second-kinetic model gives a better fit to the experimental data.

Finally, the intra-particle diffusion model plots are given in Fig. 5d. The q_t values were correlated linearly with $t^{1/2}$ values and the rate constant K_{dif} was directly evaluated from the slope of the regression line (Fig. 5d). As described by Kannan and Sundaram [54], according to this model, if the q_t vs. $t^{1/2}$ plot gives a straight line passing through the origin, then the adsorption process can be fitted by the intra-particle diffusion. The larger the intercept, the greater is the boundary layer effect. In this study, the plots of q_t vs. $t^{1/2}$ are straight lines with different intercepts. The biosorption of CV gives an intercept very close to zero and a diffusion coefficient greater than the other dyes. Hence, we can say that the biosorption process of CV was verified by the intra-particle diffusion model. However, the biosorption process of MB and BF was affected by the boundary layer as the intercepts were so far from the origin.

3.9. Thermodynamic studies

The values of $\Delta H°$ and $\Delta S°$ were deduced from lnK_d vs. 1/T plot (Fig. 5e), and Table 3 shows the values of thermodynamic parameters. As $\Delta H°$ values are positive, the process is endothermic and the dyes biosorption process was favored at higher temperatures. The negative values of $\Delta G°$ for all dyes studied indicate the feasibility and spontaneous nature of dye biosorption, while the positive values of ΔS° confirm a physical biosorption nature.

4. Conclusion

Synthetic dyes are currently used in different industries. As a result, industrial effluents are often loaded with these pollutants and represent a risk to humans and their environment. The objective of this work was the valorization of loofah, which belongs to the cucurbitaceae family and the evaluation of its performance on eliminating organic dyes (crystal violet, methylene blue and basic fuchsine) in aqueous media by biosorption. The biosorption of the dyes on loofah showed a relatively slow kinetics, the equilibrium is reached after 60 minutes of contact between the adsorbate/adsorbent with discoloration yields of 94%, 85% and 84% for crystal violet, methylene blue and basic fuchsine respectively. These results were obtained at the natural pH of the solutions (pH = 6.92 for crystal violet, pH = 6.60 for methylene blue and pH = 8.53 for basic fuchsine). The biosorption of dyes decreases with the increase of the initial concentration of dye and increases with the rise in temperature with maximum levels recorded at 60°C and which are estimated at 99.5%, 98.66%

Table 3
Thermodynamic parameters for the biosorption of dyes on loofah (C_0 = 6 mg/L, initial pH (CV = 6.92, MB = 6.60, BF = 8.53))

	MB			CV			BF		
$T°$	$\Delta G°$ (kJ/mol)	$\Delta S°$ (J/mol K)	$\Delta H°$ (kJ/mol)	$\Delta G°$ (kJ/mol)	$\Delta S°$ (J/mol K)	$\Delta H°$ (kJ/mol)	$\Delta G°$ (kJ/mol)	$\Delta S°$ (J/mol K)	$\Delta H°$ (kJ/mol)
25	−1.04			−4.87			−2.06		
40	−1.73	94.324	25.57	−5.31	494.39	138.07	−5.55	493.93	142.00
60	−2.22			−11.04			−8.57		

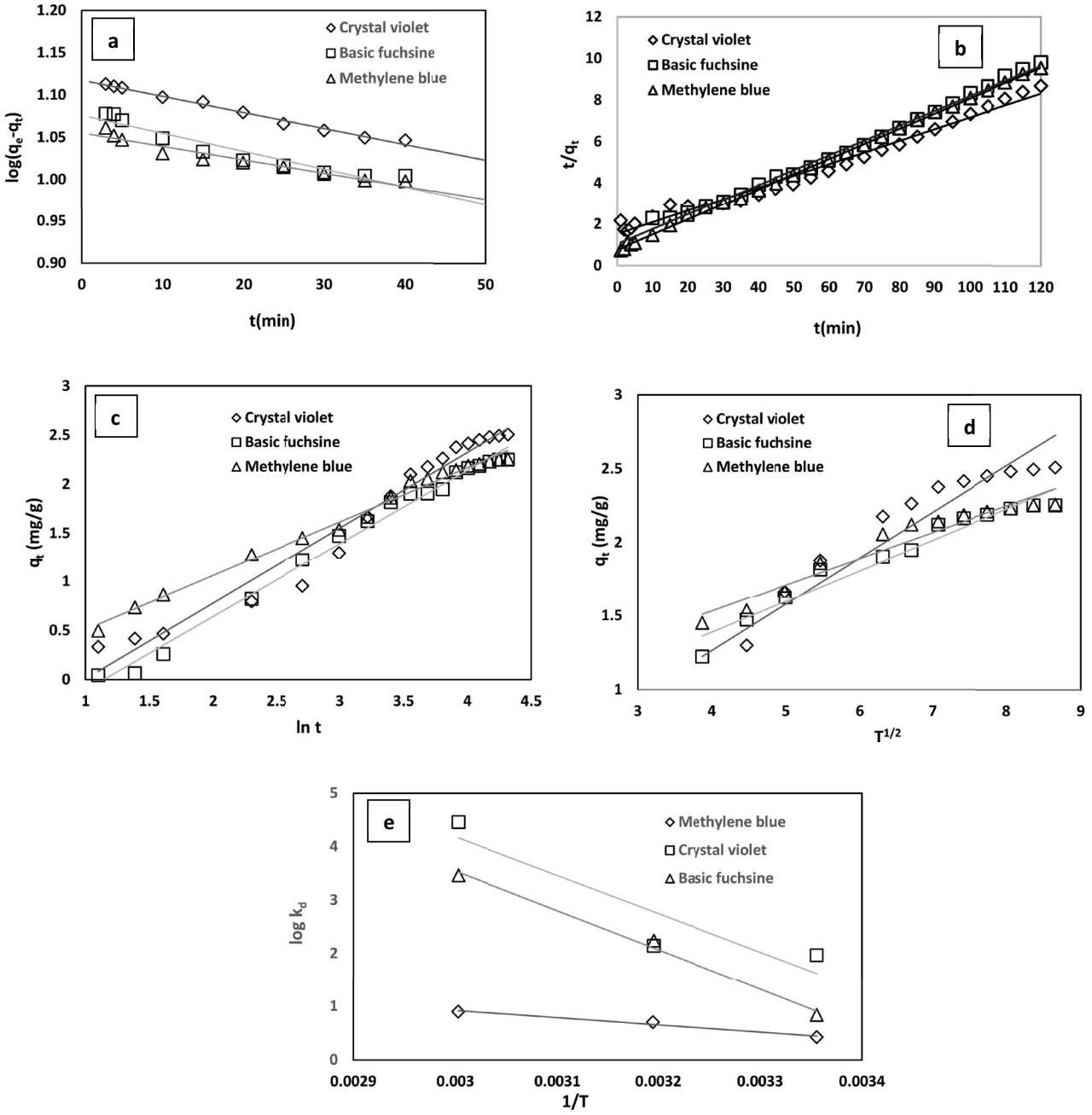

Fig. 5. Kinetic model and thermodynamic plots for biosorption of dyes on loofah: (a) first-order, (b) second-order, (c) Elovich, (d) Intra-particle diffusion, and (e) Van't Hoff equation.

and 85% for crystal violet, basic fuchsine and methylene blue respectively. The applied adsorption isotherm models showed the Langmuir isotherm model with the best fit of experimental data. The dimensionless constant R_L were found to be between 0 and 1 for all dyes used and indicates a favorable biosorption process. The kinetic studies indicated that the adsorption kinetics follow the pseudo second order. Thermodynamic studies indicate the feasibility and spontaneous nature of dyes biosorption which was favored at higher temperatures. As a result, loofah which is a green material, readily available and inexpensive, can be a cheaper alternative to commercial and more expensive materials for the removal of dyes from water.

References

[1] M.S. Chiou, H.Y. Li, Equilibrium and kinetic modeling of adsorption of reactive dye on cross-linked chitosan beads, J. Hazard. Mater., 93 (2002) 233–248.
[2] K. Vijayaraghavan, J. Mao, Y.S. Yun, Biosorption of methylene blue from aqueous solution using raw and

polysulfone-immobilized *Corynebacterium glutamicum*: batch and column studies, Bioresour. Technol., 99 (2008) 2864–2871.
[3] R. Saravanan, V.K. Gupta, V. Narayanan, Visible light degradation of textile effluent using novel catalyst ZnO/g-Mn_2O_3, J. Taiwan Inst. Chem. Eng., 45 (2014) 1910–1917.
[4] V.K. Gupta, I. Ali, T.A. Saleh, Chemical treatment technologies for waste-water recycling – an overview, RSC Adv., 2 (2012) 6380–6388.
[5] F. Rahman, The treatment of industrial effluents for the discharge of textile dyes using by techniques and adsorbents, J. Text. Sci. Eng., 6 (2016) 242–251.
[6] R. Saravanan, V.K. Gupta, E. Mosquera, Visible light induced degradation of methyl orange using β-Ag0.333V_2O_5 nanorod catalysts by facile thermal decomposition method, J. Saudi Chem. Soc., 19 (2015) 521–527.
[7] D.L. Zhao, Y. Xin, C.L. Chen, X.K. Wang, Enhanced photocatalytic degradation of methylene blue on multiwalled carbon nanotubes–TiO_2, J. Colloid Interface Sci., 398 (2013) 234–239.
[8] J.W. Lee, S.P. Choi, R. Thiruvenkatachari, W.G. Shim, H. Moon, Submerged microfiltration membrane coupled with alum coagulation/powdered activated carbon adsorption for complete decolorization of reactive dyes, Water Res., 40 (2006) 435–444.
[9] G.X. Zhao, J.X. Li, X.M. Ren, J. Hu, W.P. Hu, X.K. Wang, Highly active MnO_2 nanosheet synthesis from graphene oxide templates and their application in efficient oxidative degradation of methylene blue, RSC Adv., 31 (2013) 12909–12914.
[10] S. Coia-Ahlman, K.A. Groff, Textile wastes, J. Water Pollut. Control Fed., 62 (1990) 467–473.
[11] Z. Shen, W. Wang, J. Jia, J. Ye, X. Feng, A. Peng, Degradation of dye solution by an activated carbon fiber electrode electrolysis system, J. Hazard. Mater., 84 (2001) 107–116.
[12] L. Fan, Y.W. Zhou, W.S. Yang, G.H. Chen, F.L. Yang, Electrochemical degradation of amaranth aqueous solution on ACF, J. Hazard. Mater., 137 (2006) 1182–1188.
[13] L. Fan, Y. Zhou, W. Yang, G. Chen, F. Yang, Electrochemical degradation of aqueous solution of amaranth azo dye on ACF under potentiostatic model, Dyes Pigm., 76 (2008) 440–446.
[14] M. Tsezos, Biosorption of metals; the experience accumulated and the outlook for technology development, Hydrometallurgy, 59 (2001) 241–243.
[15] Z. Aksu, I.A. Isoglu, Use of agricultural waste sugar beet pulp for the removal of Gemazol turquoise blue-G reactive dye from aqueous solution, J. Hazard. Mater., 137 (2006) 418–430.
[16] A.A. Ahmad, B.H. Hameed, N. Aziz, Adsorption of direct dye on palm ash: kinetic and equilibrium modeling, J. Hazard. Mater., 141 (2007) 70–76.
[17] M. Hasan, A.L. Ahmad, B.H. Hameed, Adsorption of reactive dye onto crosslinked chitosan/oil palm ash composite beads, Chem. Eng. J., 136 (2008) 164–172.
[18] Z. Al-Qodah, Adsorption of dyes using shale oil ash, Water Res., 34 (2000) 4295–4303.
[19] B.H. Hameed, D.K. Mahmoud, A.L. Ahmad, Sorption of basic dye from aqueous solution by pomelo (*Citrus grandis*) peel in a batch system, Colloids Surf., A, 316 (2008) 78–84.
[20] A. Mittal, A. Malviya, D. Kaur, J. Mittal, L. Kurup, Studies on the adsorption kinetics and isotherms for the removal and recovery of methyl orange from wastewaters using waste materials, J. Hazard. Mater., 148 (2007) 229–240.
[21] J.F. Osma, V. Saravia, J.L. Toca-Herrera, S.R. Couto, Sunflower seed shells: a novel and effective low-cost adsorbent for the removal of the diazo dye reactive black 5 from aqueous solutions, J. Hazard. Mater., 147 (2007) 900–905.
[22] V.K. Gupta, R. Jain, S. Varshney, V.K. Saini, Removal of Reactofix Navy Blue 2 GFN from aqueous solutions using adsorption techniques, J. Colloid Interface Sci., 307 (2007) 326–332.
[23] V.K. Gupta, R. Jain, S. Varshney, Removal of Reactofix Golden Yellow3 RFN from aqueous solution using wheat husk – an agricultural waste, J. Hazard. Mater., 142 (2007) 443–448.
[24] V. Ponnusami, S. Vikram, S. Srivastava, N. Guava, *Psidium guajava* leaf powder: novel adsorbent for removal of methylene blue from aqueous solutions, J. Hazard. Mater., 152 (2008) 276–286.
[25] A.K. Jain, V.K. Gupta, A. Bhatnagar Suhas, Utilization of industrial waste products as adsorbents for the removal of dyes, J. Hazard. Mater., B101 (2003) 31–42.
[26] H.W. Yeung, W.W. Li, T.B. Ng, Isolation of a ribosome inactivating and abortifacient protein from seeds of *Luffa acutangula*, Int. J. Pept. Protein Res., 38 (1991) 15–19.
[27] H. Demir, A. Top, D. Balköse, S. Ulkü, Dye adsorption behavior of *Luffa cylindrica* fibers, J. Hazard. Mater., 153 (2008) 389–394.
[28] K.E. Bal, Y. Bal, A. Lallam, Gross morphology and absorption capacity of cell-fibers from the fibrous vascular system of loofah (*Luffa cylindrica*), Text. Res. J., 74 (2004) 241–247.
[29] O. Abdelwahab, Evaluation of the use of loofah activated carbons as potential adsorbents for aqueous solutions containing dye, Desalination, 222 (2008) 357–367.
[30] N.A. Oladoja, C.O. Aboluwoye, A.O. Akinkugbe, Evaluation of loofah as a sorbent in the decolorization of basic dye contaminated aqueous system, Ind. Eng. Chem. Res., 48 (2009) 2786–2794.
[31] Y. Ait Ouaissa, M. Chabani, A. Amrane, A. Bensmaili, Removal of tetracycline by electrocoagulation: kinetic and isotherm modeling through adsorption, J. Environ. Chem. Eng., 2 (2014) 177–184.
[32] I. Langmuir, The adsorption of gases on plane surfaces of glass, mica and platinum. J. Am. Chem. Soc., 40 (1918) 1361–1403.
[33] K.R. Hall, L.C. Eagleton, A. Acrivos, T. Vermeulen, Pore- and solid-diffusion kinetics in fixed-bed adsorption under constant-pattern conditions, Ind. Eng. Chem. Fundam., 5 (1966) 212–223.
[34] M.J. Temkin, V. Pyozhev, Recent modifications to Langmuir isotherms, Acta Physicochim., USSR, 12 (1940) 327–352.
[35] M.M. Dubinin, E.D. Zaverina, L.V. Radushkevich, Sorption and structure of active carbon, J. Phys. Chem., 21 (1947) 1351–1362.
[36] S. Lagergren, Zur threorie der sogenannten adsorption gelosterstoffe, Kungliga svenska vetenskapsakademiens, Handlingar., 24 (1898) 1–39.
[37] Y.S. Ho, G. McKay, D.A.J. Wase, C.F. Foster, Study of the sorption of divalent metal ions on to peat, Adsorpt. Sci. Technol., 18 (2000) 639–650.
[38] S.H. Chien, W.R. Clayton, Application of Elovich equation to the kinetics of phosphate release and sorption on soils, Soil Sci. Soc. Am. J., 44 (1980) 265–268.
[39] W.J. Weber, J.C. Morris, Kinetics of adsorption on carbon from solution, J. Sanit. Eng. Div. ASCE, 89 (1963) 31–59.
[40] H.B. Senturk, D. Ozdes, C. Duran, Biosorption of Rhodamine 6G from aqueous solutions onto almond shell (*Prunus dulcis*) as a low cost biosorbent, Desalination, 252 (2010) 81–87.
[41] R.F. Nascimento, A.C.A. Lima, A.B. Vidal, Adsorption: Theoretical Aspects and Environmental Applications, Fortaleza, Imprensa Universitària, 2014.
[42] D.L. Pavia, G.M. Lampman, G.S. Kriz, Introduction to Spectroscopy, Cengage Learning, Sao Paulo, 2010.
[43] V.O.A. Tanobe, T.H.D. Sydenstricker, M. Munaro, S.C.A. Amico, comprehensive characterization of chemically treated Brazilian sponge-gourds (*Luffa cylindrica*), Polym. Test., 24 (2005) 474–482.
[44] S.E. Olaseni, N.A. Oladoja, O. Olanrewaju, O. Christopher, O. Medinat, Adsorption of Brilliant Green onto *Luffa cylindrical* sponge: equilibrium, kinetics, and thermodynamic studies, ISRN Phys. Chem., 8 (2014) 1–12.
[45] C.F. Iscen, I. Kiran, S. Ilhan, Biosorption of Reactive Black 5 dye by *Penicillium restrictum*: the kinetic study, J. Hazard. Mater., 143 (2007) 335–340.
[46] J.F. Osma, V. Saravia, J.L. Toca-Herrera, Sunflower seed shells: a novel and effective low-cost adsorbent for the removal of the diazo dye Reactive Black 5 from aqueous solutions, J. Hazard. Mater., 147 (2007) 900–905.
[47] M.C. Ncibi, B. Mahjoub, M. Seffen, Kinetic and equilibrium studies of methylene blue biosorption by *Posidonia oceanica* (L.) fibres, J. Hazard. Mater., B139 (2007) 280–285.

[48] A.F. El-Nagawy, M.S. Abdo, H.A. Farag, A.A. Farag, G.H. Sedahmed, Diffusion of dyes in electrolyte solutions across aboundary, Indian J. Technol., 16 (1978) 454–462.
[49] B. Yu, Y. Zhang, A. Shukla, S.S. Shukla, K.L. Dorris, The removal of heavy metal from aqueous solutions by sawdust adsorption – removal of copper, J. Hazard. Mater., B80 (2000) 33–42.
[50] P.K. Malik, Dye removal from wastewater using activated carbon developed from sawdust: adsorption equilibrium and kinetics, J. Hazard. Mater., 113 (2004) 81–88.
[51] L. Khezami, R. Capart, Removal of chromium (VI) from aqueous solution by activated carbons: kinetic and equilibrium studies, J. Hazard. Mater., 123 (2005) 223–231.
[52] Y.S. Ho, G. McKay, Sorption of dye from aqueous solution by peat, Chem. Eng. J., 70 (1998) 115–124.
[53] A.S. Ozcan, B. Erdem, A. Ozcan, Adsorption of Acid Blue 193 from aqueous solutions onto BTMN-bentonite, Colloids Surf., A., 266 (2005) 73–81.
[54] K. Nagarethinam, M.S. Mariappan, Kinetics and mechanism of removal of methylene blue by adsorption on various carbons — a comparative study, Dyes Pigm., 51 (2001) 25–40.